

Jacobs Journal of Hydrology

Research Article

The Study of Intensity, Duration and Type of Thunderstorms using Radar Images and Instability Indices in Southwest of Iran (Case Studies)

Foroozan Arkian^{*1}, Sajad shahheidari¹

¹Meteorology Department, Marine Science and Technology Faculty, Tehran North branch, Islamic Azad University, Iran

^{*}Corresponding author: Dr. Foroozan Arkian, Marine Science and Technology Faculty, Zafaraniyeh Street, Tehran, Iran

Email: f.arkian@gmail.com; Tel: +989125805886; Fax: +982122404843

Received: 06-22-2015

Accepted: 08-19-2015

Published: 09-05-2015

Copyright: © 2015 Foroozan

Abstract

Thunderstorms produce damaging winds, hail and shower over southwestern Iran during the cold season. We tried to obtain knowledge of Intensity, Duration and Type (IDT) of the storms by radar images and some convection-related parameters such as K, Showalter, Total Total, Helicity and Energy-Helicity (EHI) indices; Convective available potential energy (CAPE) and Bulk Richardson number (BRN) in the area. The surface and upper air data were taken from General Forecast System (GFS) with spatial resolution of $0.5^{\circ} \times 0.5^{\circ}$ and a temporal resolution of 6 h. The case studies consist three convective systems that caused severe damage and flooding in the area.

By examining thunderstorms (containing 66 cells) via analysis of radar reflectivity image and instability indices, practically, super cell with tornado sign, single cell and multicellular are 14 %, 48.5 % and 37.5 %, respectively. Convective cells with quick horizontal movement have significant wind shear between $15\text{-}24 \text{ ms}^{-1}$. Vertical Integrated Liquid (VIL) was calculated more than 50 kg m^{-2} for all convective cells accompanied by hail.

Keywords: Southwestern Iran; Thunderstorms Type; Weather Radars; Max Radar Reflectivity; Instability Indices

Abbreviations:

IDT: Intensity Duration and Type of the Storm;

EHI: Energy- Helicity index;

CAPE: Convective Available Potential Energy;

BRN: Bulk Richardson Number;

GFS: General Forecast System;

TOR: Tornadic Super-cell;

SUP: Super-cell;

ORD: Single cell;

MUL: Multi-cell;
SRH: Storm-Relative Helicity;
PW: Precipitation Water of cloud;
SI: Showalter stability Index;
TTI: Total Total Index;
VWS: Vertical Wind Shear;
CTR: Cell Centroid Tracking;
VIL: Vertical Integrated Liquid.

Introduction

The knowledge of thunderstorms characteristics is necessary for short term forecasting and long term planning in southwest of Iran near to Zagros ranges (mountains). A line of thunderstorms rises along Zagros Mountains edge due to moisture air lifting. Therefore, knowing the formation mechanism of the thunderstorms can be helpful to reducing agricultural damages in the area.

Thunderstorms include different type such as Ordinary (ORD), Multi cell (MUL), super cell (SUP), Tornado (TOR) and squall line. Knupp and Stalker [1] investigated multi-cell thunderstorms using some indices such as convective available potential energy, diluted updraft, cloud-layer depths, updraft area and radar images. Byko et al [2]. studied downdraft reflectivity cores in SUP thunderstorms with high-resolution mobile radar and numerical simulation. Cores of downdraft lead to observe increasing circulation in low-level before full development in SUP thunderstorm. Downdraft cores are flooded to right posterior of storms and in occur dance with small-scale main radar reflection. They helped to form a Hook Echo while observing them in radar reflection and reaching to low levels.

Sounding climatologies have also been used to assess the environments related to particular types of thunderstorms. Bluestein and Parks [3] utilized soundings to compare the environments of low-precipitation storms and classic supercells, and Rasmussen and Straka [4] investigated these and high-precipitation supercells using a sounding climatology. Bluestein and Parker [5] have used soundings to investigate the modes of early storm organization near the dryline. A climatological sounding analysis of the environments associated with severe Oklahoma squall lines is reported in Bluestein and Jain [6] and non-severe squall lines in Bluestein et al [3]. Salehi et al [7]. investigated vertical structure of severe thunderstorms in north-eastern Iran.

Rasmussen and Blanchard [4] examined all of the 0000 UTC

soundings from the United States made during the year 1992 that have nonzero convective available potential energy (CAPE). Soundings are classified as being associated with nonsupercell thunderstorms, supercells without significant tornadoes, and supercells with significant tornadoes. This classification is made by attempting to pair, based on the low-level sounding winds, an upstream sounding with each occurrence of a significant tornado, large hail, and/or 10 or more cloud-to-ground lightning flashes. Severe weather wind parameters (mean shear, 0–6-km shear, storm-relative helicity, and storm-relative anvil-level flow) and CAPE parameters (total CAPE and CAPE in the lowest 3000 m with buoyancy) are shown to discriminate weakly between the environments of the three classified types of storms. In the similar research, Arkian and Karimkhani [9] have determined the type of flood producing thunderstorms by some convective related parameters and radar images in northeast of Iran.

In this research we try to find the type of thunderstorms that produce severe shower and destructive hail in southwestern of Iran. We've used Reflectivity and Vertically Integrated Liquid (VIL) product of radar for determination of the intensity, duration and type (IDT) of thunderstorms. Since, Reflectivity of radar is not sufficient to identify thunderstorm types, we've calculated some instability indices such as showalter index, K index, Total Total index, Convective available potential energy (CAPE), Bulk Richardson number (BRN), Helicity, Energy-Helicity index, Vertical wind shear and Precipitable water (PW). However, no known baseline exists that is adequate to support these quantifications in the different area such as ours region, we tried to find type of storms with preset threshold of the parameters and then verify them with our observation from storms and compare them with the result of Rasmussen and Blanchard [4] paper.

Materials and method

Severe thunderstorm codes (80 to 99) was extracted from the dataset of twenty synoptic and agricultural standard weather stations for 2007-2013 years in southwest of Iran (Khuzestan province). Furthermore, insurance offices and disaster task force has confirmed the storms that produced destructive large hail, lighting and severe shower in the area. In this study, three cases was chosen in 2010, 2011 and 2013. Surface and upper air data were taken from General Forecast System (GFS). These data have a spatial resolution of $0.5^{\circ} \times 0.5^{\circ}$ and a temporal resolution of 6 h. Also, the soundings compared here are contained in Radiosonde Data for southwestern Iran, and were all made at 1200 UTC formal sounding. The dataset containing some sounding-derived parameters such as K, Showalter, Total-Total, Helicity and Energy-Helicity (EHI) indices; Convective Available Potential Energy (CAPE) and Bulk Richardson Number (BRN) are used for detect type of thunderstorms.

The radar data used in this study were reflectivity scans from

S-band radar. From low to high level 360° scans at elevation angles of 0.5° and 19.5° were obtained every 15 min out to a range of 250 km. The S-band radar characteristic is listed in Table. 1. These surveillance scans were used to identify structure of cumulus clouds in their early development stage prior to precipitation. We have used radar images for identify IDT of thunderstorms.

The classes of storm are Single-cells, Multi-cells, Super-cell, Tornadoic Super-cells and Squall line storms. These categories of storms (convective cells) were defined as bellow:

Tornadoic Super-cell (TOR): This category was designed to identify soundings associated with tornadoic Super-cells. Super-cell (SUP): For comparison to the TOR category, information from the climatological database was sought to identify Super-cells without significant tornadoes.

Single-cell (ORD): This category was designed to exclude Supercells. This was done by including soundings associated with a modest amount of cloud-to-ground lightning, but excluding soundings associated with damaging wind, large hail, or any tornado.

Multi-cell (MUL): Multicellular organisms are organisms that consist of more than one cell, in contrast to single-celled organisms. To form a multicellular organism, these cells need to identify and attach to the other cells.

Complex cells (clusters): This category has been organized into two or more single cells that merge together. Squall line: This category associated with ensemble of single/Multi /Super-cells that accompanied with a cold front.

The studied area (Khuzestan province) can be basically divided into two regions, the rolling hills and mountainous regions north of the Ahwaz Ridge, and the plains and marsh lands to its south. The climate of Khuzestan is generally hot and occasionally humid, particularly in the south, while winters are much more cold and dry. Summertime temperatures routinely exceed 40 degrees Celsius and in the winter it can drop below freezing, with occasional snowfall, all the way south to Ahwaz.

Ahwaz weather radar works in S Doppler frequency band and is used for short-term forecasting, rainfall flood and road and aviation.

Case Study (2 November 2010)

The convective cells was triggered in the north of Khuzestan province (32.16° N, 48.25° E, Sea level height 82m) with sever lightning, high wind, showering at 18:00 UTC until early next morning. The maximum rainfall in the some stations was exceed to 54 mm/day. Also, sever hail shower was reported in

the some villages with baseball-size that made agricultural damage, cars and head injury. Hourly and daily precipitation (DP) of Khuzestan province listed in Table. 2.

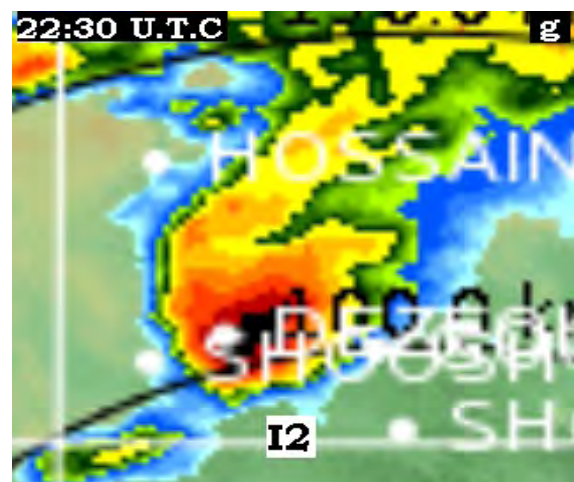
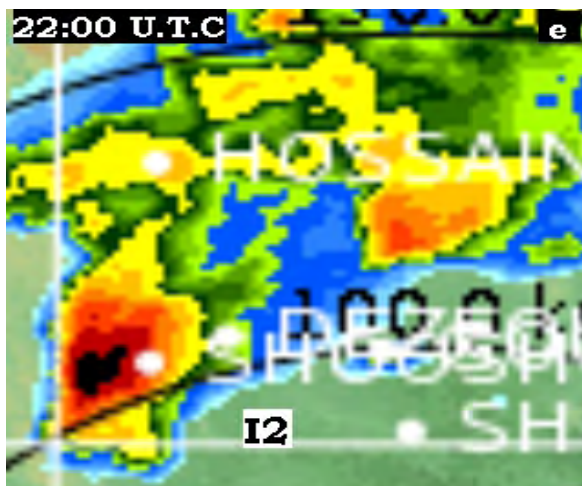
Table. 1. Characteristic of S-band radar

1	Radar model	Metero 1500 s	6	Antenna range	250 km
2	H Rotation Angle	0~360°	7	Antenna diameter	11.5 m
3	V Rotation angle	-2~180°	8	Radar mast height	24 m
4	Sea level height	24.5 m	9	Position stabilization accuracy	0.1°±
5	Altitude	30 m	10	H/V rotation speed	1~36°

Radar images were produced by Rainbow software in 15 min intervals and the convective cell is identified based on their radar Max reflectivity by considering 40dBz threshold [8]. Fig. 1 shows hook echo formation on 2 November 2010. Hook echo detection is sensitive to the space and time resolutions of the radar. The idea that a hook echo forms as hydrometeors from a super cell's main echo region are advected toward the rear of the storm by the rotating updraft seems to have been widely accepted, although Lemon [10] and Rasmussen et al [4]. Have documented hook echoes that form when reflectivity cores descend from aloft to low levels on the rear flank of the storm, initially detached from the main echo at low levels, and subsequently become connected to the main echo to form a hook echo. These observations suggest that hook echoes might not always form from the simple horizontal advection process envisioned by Browning [11] and Fujita [12]. Of course, the evolution of the reflectivity field is never solely a result of the horizontal advection of precipitation anyway, because hydrometeors fall relative to the air; that is, hook-echo formation inescapably involves descending precipitation curtains. Thus, the question is not whether the descent of precipitation cores can contribute to hook-echo formation, but whether a spectrum of hook-echo formation exists, whereby the horizontal advection of precipitation might dominate the evolution of the low-level reflectivity field and formation of some hook echoes at one end of the spectrum (as in the studies by Fujita [12] and Browning [11]) and hydrometeor fall speeds dominate the evolution of the low-level reflectivity field and hook-echo formation at the other end of the spectrum (as in the cases documented by Rasmussen et al. [4]).

Table 2. Hourly and daily precipitation in the synoptic stations of Khuzestan province during 1-3 November 2010.

Significant Phenomenon										
Stations	2/11/2010					3/11/2010				
	00	06	12 UTC	18 UTC	DP(mm)	00 UTC	06 UTC	12 UTC	18 UTC	DP(mm)
Dezful			29	97	35.6	97	01			18.6
Bostan				17	0.0	29				3.5
Ahwaz					0.0	95				6.9
Masjed Soleiman			17	95	31.2	17				3.4
Ramhormoz					0.0		95			14.4
Abadan					0.0					0.0
Mahshahr					0.0					0.0
Omidieh					0.0		95			7.2
Behbahan					0.0		95	29		5.1
Shushtar			17		0.0		29			2.7
Ezeh			13		0.0		29	29		4.9
Shadegan					0.0					0.0
Hosseinieh					0.0	25	13			14.3
Lali			80	29	0.0	95				7.0
Gotvand			29	17	3.0	97				3.0
Susa			17	29	0.0	99				43.0
Dehdez					0.0		95			4.9
Agriculture Ahwaz					0.0	17	29			28.4
Hendijan					0.0		96			34.4
Aghajari					0.0					0.0



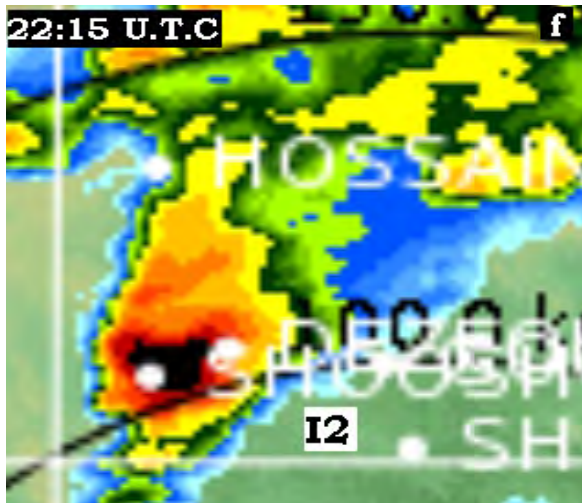


Figure 1. Hook Echo formation on 2 November 2010.

Results show that the reflectivity core intensity and vertical growth must exceed 60 dBZ and 15 km for hail event, respectively. Also, VIL was estimated about 50 kg m⁻² for hailstorm and often very high or increasing. Subsequently, values slowly subsided to 50 kg m⁻² when baseball-size surface hail and violent winds were actually being reported. High values of VIL and pronounced three-body scattering very often precede surface hail falls. VIL has predictive value in that it often develops during hail growth aloft and before very large hail reaches the surface. With the correlation of very large hail and often violent winds with the most striking signatures, in these cases VIL detection should suggest stronger wording in the resulting warning. The convective cells have relative quick movement in CTR images and move toward North East. Vertical growth of cells indicates high updraft strength and their movement is related to vertical wind shear [9].

Instability indices calculation

In this research, some instability indices such as KI, SI, TTI, CAPE, PW, BRN, SRH, EHI, VWS were calculate by using Skew-T diagram and General Forecasting Model (GFS) data for identify the type of storms. Here is some indices definitions:

Storm-Relative Helicity (SRH)

SRH is sounding-derived shear parameter Davies-Jones et al. [13] that defined as:

$$SRH = \int_0^h k \cdot (v - c) \times \frac{\partial v}{\partial z} dz \quad (1)$$

Where V is horizontal velocity, c is the storm motion vector, and h is the depth over which the integration is performed (3

km herein) and SRH unit is m²/s². Table 3 shows SRH values for different percentile in soundings associated with non-super-cell thunderstorms (ORD), supercells without significant tornadoes (SUP), super-cells with significant tornadoes (TOR).

BL-6 km shear

In this section, the magnitude of the shear vector between the 0–500 m AGL mean wind and 6 km AGL wind (hereafter BL–6-km shear) is examined and shear unit is ms⁻¹. Table. 3 shows the frequency of occurrence of various magnitudes of BL–6 km shear as a function of category.

Convective Available Potential Energy

CAPE Moncrieff and Miller [14] is in common use as a forecast tool for super-cells and it unit is Jkg⁻¹. Table. 3 shows values of CAPE for ORD, TOR and SUP. Interestingly, CAPE is significantly different between ORD and SUP soundings, as well as between ORD and TOR soundings, suggesting that CAPE alone has some value as a super cell predictor, even when not paired with a measure of shear, although combined measures are much better.

Bulk Richardson number

The Bulk Richardson Number is calculated as follows:

$$BRN = \frac{CAPE}{(0.5 \times (U_{6 \text{ km}} - U_{500 \text{ m}})^2)} \quad (2)$$

The bulk Richardson number (BRN) has been used as a super-cell predictor ever since it was investigated using numerical simulations Hart and Korotky [15]. Weisman and Klemp (1982) determined that environments with BRN>50 favored multicellular events.

Energy– Helicity index

The Energy–Helicity index (EHI) [16,17] is defined as:

$$EHI = \frac{CAPE \times SRH}{1.6 \times 10^5} \quad (3)$$

This index is used operationally for super-cell and tornado forecasting, with values larger than 1.0 indicating a potential for supercells, and EHI .2.0 indicating a large probability of super-cells. The likelihood of significant tornadoes does increase with increasing EHI, as shown in Table. 3.

Table 3. Percentile of some indices for soundings associated with nonsuper-cell thunderstorms (ORD), supercells without significant tornadoes (SUP), supercells with significant tornadoes (TOR), [4].

Parameter	ORD Percentile			SUP Percentile			TOR Percentile		
	10	25-75	90	10	25-75	90	10	25-75	90
BL-6km shear	3-5.7	5.7-15.7	15.7-22	8.1-12.1	12.1-22.1	22.1-25.8	4.7-13.6	13.6-21.8	21.8-29
BRN	0.19-1.5	1.5-40	40-140	0.94-2.0	2.0-17.3	17.3-34	1.13-4.2	4.2-13.7	13.7-20.8
SRH	-19	17-100	100-168	25-64	64-208	208-304	68-100	100-279	279-411
Mean shear (0-4 km)	2.79-3.61	3.61-6.42	6.42-8.09	4.52-5.23	5.23-7.83	7.83-9.44	4.52-5.06	5.06-9.44	9.44-10.29
CAPE	-	0-1094	1094-1821	0-283	283-1821	1821-2453	66-519	519-1877	1877-3028

Table 4. Radar survey and instability indices for selected cases.

cell name	Radar images		BRN	CAPE	Wind Shear (m/s)	SRH	EHI	TTI	KI	SI	Type	Intensity	PW (kg/m2)	
	Movement	Vertical growth (km)												
02/11/2010	A	✓	10	1.5	400	15.5	267	0.53	42.6	14.9	4.34	single-cell	70	17.8
	G	✓	15	0.6	550	14.5	174	0.27	42.6	14.9	4.34	super-cell	70	16.8
	I1	✓	10	0.9	150	15.6	250	0.44	42.6	14.9	4.34	single-cell	70	17.75
	I2	✓	15	0.7	100	15.6	264	0.46	42.6	14.9	4.34	super-cell	70	17.75
	J	✓	15	0.5	130	17	215	0.36	42.6	14.9	4.34	super-cell	70	17.75
02/11/2011	C	✓	15	1.5	400	23.5	150	0.38	57	36	-2	super-cell	70	16.5
	K	✓	10	2.5	550	23	80	0.28	57	36	-2	single-cell	70	17.5
	O-B1-G	✓	10	0.8	150	19	165	0.15	57	36	-2	multi-cell	70	18.5
	A2-Q-R-S-L	✓	10	0.9	100	19.5	170	0.11	57	36	-2	multi-cell	55	19
	U	✓	15	0.5	130	28	150	0.12	57	36	-2	super-cell	70	18.7
	Y	✓	15	0.3	50	20.5	140	0.04	57	36	-2	super-cell	70	16.5
	AD	✓	12	0.3	100	24.3	150	0.09	57	36	-2	super-cell	70	17
AE	✓	5	0.5	100	22	100	0.06	57	36	-2	single-cell	70	16	
02/05/2013	A	✓	10	>100	120	8	115	0.09	54	36.5	-5	multi-cell	55	24
	CDGEFHIJ	✓	10	>100	130	7	75	0.06	54	36.5	-5	multi-cell	55	24
	N	✓	10	>100	900	12	110	0.62	54	36.5	-5	multi-cell	40	24
	M1	✓	10	>100	600	5	80	0.30	54	36.5	-5	single-cell	50	23
	M2	✓	10	>100	1100	6	120	0.83	54	36.5	-5	multi-cell	50	24
	P2	✓	10	>100	300	7.5	80	0.15	54	36.5	-5	multi-cell	70	24
	R	✓	5	>100	420	4	78	0.20	54	36.5	-5	single-cell	50	25
	Q	✓	10	>100	620	2.5	0	0.00	54	36.5	-5	multi-cell	70	25
	RT	✓	10	>100	700	2	0	0.00	54	36.5	-5	multi-cell	50	23
	U	✓	15	>100	750	0.4	0	0.00	54	36.5	-5	super-cell	70	22
Y	✓	15	>100	450	1	80	0.23	54	36.5	-5	super-cell	70	23	

Instability indices of three cases (2 November 2010, 6 November 2011 and 2 May 2013) listed in table. 4. Each cases are including several convective cells that named using Alphabet, for example, there are five convective cells (A, G, I1, I2, J) in case 1.

For identification of convective cells, all mentioned instability indices was calculated and they was compared with their own threshold in Table. 3 [4].

PW was calculated by GFS data for all convective cells. PW threshold is 8 kg/m^2 for precipitation potential of cloud [18] and according to Table. 4 in all studied cases, PW is more than the threshold. K index, and TT index indicated high instability and high probably of thunderstorms, but SI didn't show instability in some cases. The result show different type of thunderstorms such as ORD, MUL and SUP in 2 Nov 2010 and 2011 and 05 May 2013 (Table. 4).

Discussion and conclusion

Three convective systems were studied to identify IDT of violent thunderstorms by radar images and instability indices in southwest of Iran. One of our criterion for choosing the type of thunderstorm was vertical structure and reflectivity of convective cells in radar images. Since, the radar images are not sufficient for thunderstorm identification, we also have calculated some instability indices for all cells and compare them with Table. 3 [4] to identify the exact type of thunderstorms.

The amount of CAPE and component indices such as BRN and EHI in our area was lower than listed thresholds in Table. 3, therefore, determination of thunderstorms types by mentioned indices was not easy. The results show that the most thunderstorms are single cell in the coverage area of the S-band radar. By examining thunderstorms (containing 66 cells), practically, super cell with tornado sign, single cell and multicellular are 14%, 48.5% and 37.5%, respectively.

The results show that there is a direct relation between vertical growth of cells and vertical wind shear (VWS) in the radar image. The intensity changed between 40 to 70 dBz and duration time of cells was between 30 to 405 min. Convective cells with quick horizontal movements in radar images have significant wind shear between $15\text{-}24 \text{ ms}^{-1}$. VWS in layer between 500-6000 m and SRH with compare to Rasmussen and Blanchard [4] thresholds imply for identify the storm types. Applying each of indices individually to determination of cell type is not adequate and at less 4 indices shows the exact type of storm. VIL was calculated more than 50 kg m^{-2} for all convective cells accompanied by hail.

References

1. Stalker R, Knupp J, Kevin R. A Method to Identify Convective Cells Within Multicell Thunderstorms from Multiple Doppler Radar Data. *Monthly Weather Rev.* 2001, 130.
2. Byko Z, Richardson Y, Markowski P, Wurman J, Adlerman E. Descending Reflectivity Cores in Supercell Thunderstorms Observed by Mobile Radars and in a High-Resolution Numerical Simulation. *Jour of American Meteo Soci Weather & Foreca.* 2009, 24(1): 155-186.
3. Marx GT, Jain MH, Bluestein HB. Formation of mesoscale lines of precipitation: Nonsevere squall lines in Oklahoma during the spring. *Mon Weather Rev.* 1987, 115(11): 2719-2727.
4. Rasmussen N E, Blanchard O D. Baseline Climatology of Sounding-Derived Super cell and Tornado Forecast Parameters, Weather and Forecasting. Coo Institute for Meso Meteo Studies. National Sever Storms Lab and Uni of Oklahoma. Norman, Oklahoma. 1998, 13.
5. HB. Parker SS. Modes of isolated, Severe Convective Storm Formation along the Dry line. *Mon Weather Rev.* 1993, 121(5): 1354-1372.
6. Bluestein HB, Jain MH. Formation of mesoscale lines of precipitation: Severe squall lines in Oklahoma during the spring. *Jour Atmos Sci.* 1985, 42(16): 1711-1732.
7. Salehi H, Sanaee Nejhada H, Mosavi Bayegi M. Investigate damaging convective phenomena based on the analysis of the vertical structure of the atmosphere in Mashhad, The first national conference on climate in Iran, University Graduate industrial and high-tech, Iran, Kerman. 2013.
8. Nazrul Islam M d, Uyeda H, Kikuchi O, Kikuchi K. Convective and Stratiform Components of Tropical Cloud Clusters in Determining Radar Adjusted Satellite Rainfall during the TOGA-COARE IOP. *Jour Fac Sci Hokkaido Univ. Ser VII (Geophysics).* 1998, 11(1): 265-300.
9. Arkian F, Karimkhani M. Determination of The Type of Flood-Producing Thunderstorms by Convection-Related Parameters and Radar Images in Northwestern Iran. *Jour Clim & Weather Foreca.* 2014, 2(2).
10. Lemon L R. The flanking line, a severe thunderstorm intensification source. *J Atmos Sci.* 1976, 33(4), 686-694.
11. Browning K A. Airflow and precipitation trajectories within severe local storms which travel to the right of the winds. *J Atmos Sci.* 1964, 21(6): 634-639.
12. Fujita T T. Mesoanalysis of the Illinois tornadoes of 9 April 1953. *J Meteor.* 1958, 15(3): 288-296.
13. Doswell CA, Davies-Jones R, Keller DL. On summary measures of skill in rare event forecasting based on contingency tables. *Weather Forecast.* 1990, 5(4): 576-585.
14. Moncrieff M, Miller MJ. The Dynamics and Simulation of Tropical Cumulonimbus and Squall lines. *Q J Roy Meteor Soc.* 1976 102: 373-394.
15. Hart J, Korotky W. The Sharp Workstation v1.50 Users guide. National Weather Service. 1991.

16. Weisman, Klemp. On the reliability of hook echoes as tornado indicators. *Mon Wea Rev.* 1981, 109(7): 1457-1466.
17. Davies JM. Hourly Helicity, Instability, and EHI in forecasting supercell tornadoes. 1993.
18. Sadeghi Hosseini A, Rezaian M. Examination the number of indicators and the potential of seeding clouds with convective instability of the Esfahan region. *Physics of the Earth and Space Jour.* 2006, 83: 32-98.